4 Indonesia – convection and tropical plume

4.1 Reasons for selection of the case

The Indonesian Archipelago deserves special interest due to the appearance of a peculiar tropical circulation system, the so-called Walker circulation, for which the archipelago plays an important role. The trades transport warm moist air towards the Indonesian region where the sea normally is very warm. Moist air then rises to high levels of the atmosphere and travels eastward before sinking over the eastern Pacific Ocean. It is also involved in the generation of El Niño events in the Pacific Ocean which have a strong impact on the global circulation.

To study this region more intensively with CRISTA-2 a special mode of measurement, the "Hawk-eye mode", was used from August 10 – 13, 1997. In this way the density of observations was increased by a factor of 3 – 6 and it became possible to identify more details of the atmospheric structure than usual (Offermann et al. 2001). Previous and ongoing analyses of the observations revealed that a large intrusion of dry extratropical air into the tropics occurred south of Indonesia during the CRISTA episode (Offermann et al. 2001, Offermann et al. 2002) while a tropical plume (TP) formed extending as far as Australia. TPs are usually characterised by continuous bands of high or intermediate level clouds, which extend poleward and eastward from the tropics towards the subtropics or mid-latitudes (McGuirk et al., 1987). Yet in this case cloud formation as seen by CRISTA-2 was not very pronounced (Spang et al., 2002). TPs in the Australian region have been analysed by Kuhnelt (1990).

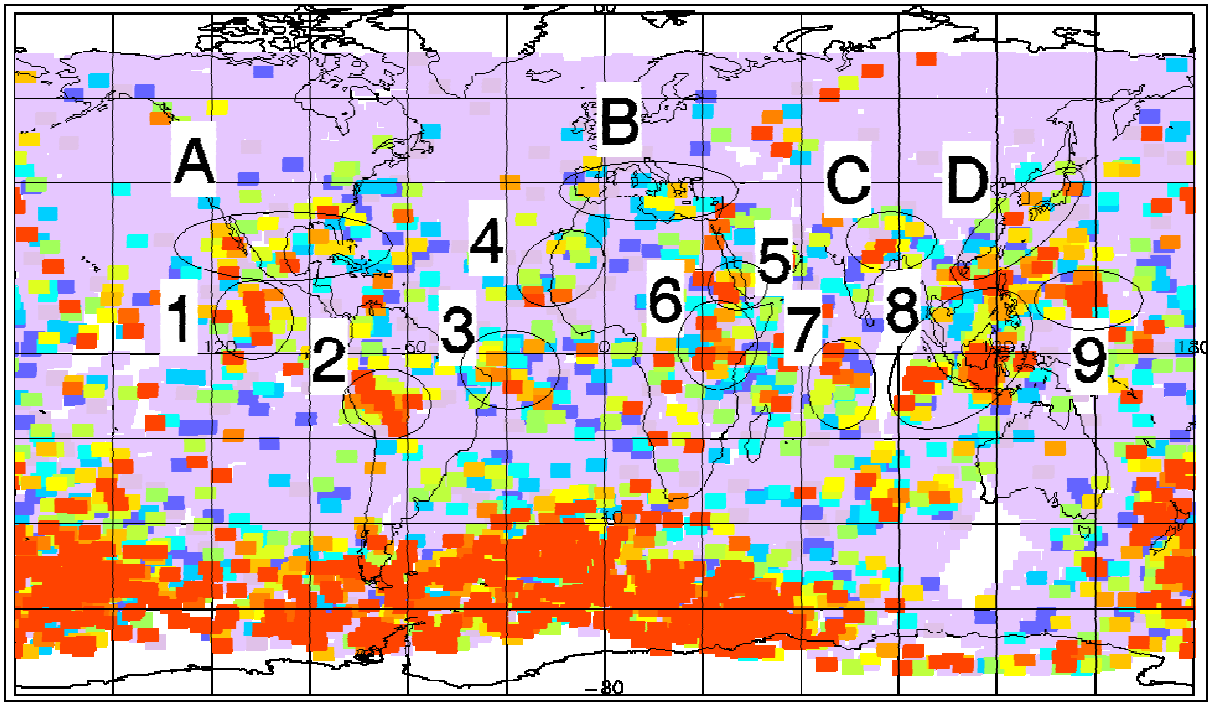

Figure 4.1: Regions of enhanced internal gravity wave activity in the stratosphere at 25 km altitude. Derived from CRISTA-2 temperature observations by Preusse (2001). Region 8 with Indonesian Archipelago.

In addition, the convective activity of the Indonesian region is clearly reflected by an increase of the intensity of gravity waves in the stratosphere as shown by Preusse (2001) by means of CRISTA observations (Fig. 4.1). This means that tropical convective systems establish a source of momentum for the middle atmosphere and thus can exert control of the circulation and tracer transport at higher levels. Furthermore, Kley et al. (2000) have pointed to the problem that mesoscale features of water vapour distribution in the upper tropical troposphere, in particular, are largely unexplored and that their role for the atmospheric water budget is badly known. It was therefore decided to exploit the existence of the special CRISTA data set for the Indonesian Archipelago and include a numerical experiment with the EURAD model system to test its applicability to the tropics and its capability of reproducing mesoscale structures as seen in the observations.

4.2 Comparison of horizontal distribution of water vapour in the upper troposphere as revealed by globally assimilated observations and regional simulations

Fig. 4.2 and 4.3 (middle right panel) exhibit the water vapour distribution on August 12, 1997, 00 UTC, as revealed by CRISTA measurements assimilated into the global NCAR/ROSE model (Rose and Brasseur, 1989; Riese et al., 1999) at 215 hPa and a regional simulation with the EURAD model system, respectively, at the same pressure level. The regional simulation employs boundary and initial values from ECMWF analyses. Obviously, the larger scale features, i. e. the big patch of dry air south of Sumatra and Java surrounded by moist air

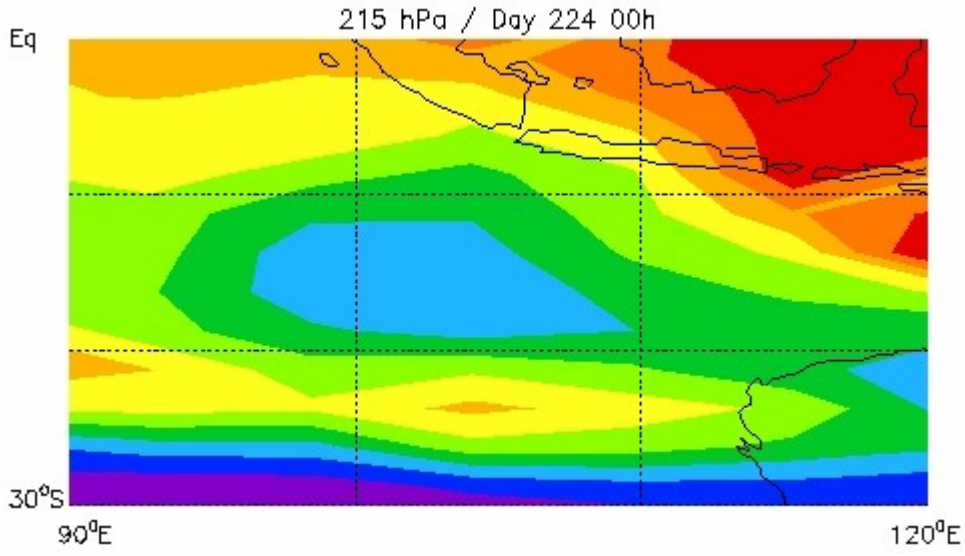

Figure 4.2: Intrusion of dry air (blue) into the tropical troposphere south of Java and Sumatra and tropical plume (band of moist air, light green to orange) west of Australia. Contours of water vapour mixing ratio in steps of 11 ppmV, purple below 22, blue 33 – 44, orange 77 – 88, dark red above 99 ppmV. From an assimilation of CRISTA observations with the NCAR Rose model, August 12, 1997, 00 UTC (Offermann et al., 2002)

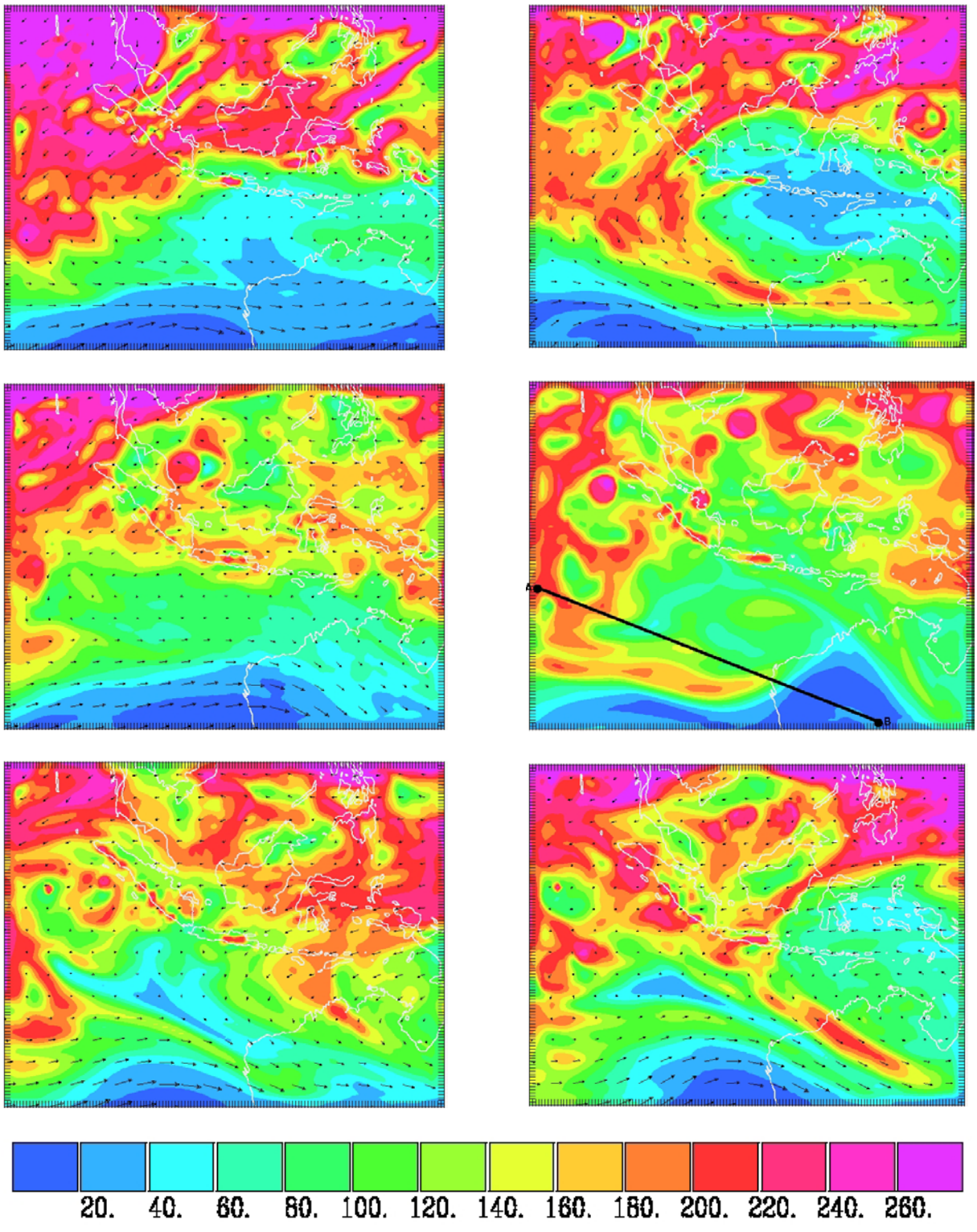

Figure 4.3: Water vapour mixing ratio [ppm] and horizontal wind [m/s] at 215 hPa. From upper left to lower right: 4 August, 00 UTC, 6 August, 00 UTC, 10 August, 00 UTC, 12 August, 00 UTC, 14 August, 00 UTC, 16 August, 00 UTC. Map of 12 August shows the position of the vertical cross section in Fig. 4.4

masses and an elongated tongue of moist air west of North Australia (the tropical plume) are grossly similar. Yet the regional simulation with higher resolution than the original measurements and the global model gives clear evidence that considerable fine structure exists in the analysed region as it can be expected from the well known fact that strong convection usually exists in this area. The findings of Preusse (2001) regarding increased gravity wave activity over Indonesia as shown in Fig. 4.1 are an indirect indication that the regional model realistically reproduces the behaviour of the tropical troposphere on the meso-scale.

The evaluation of EURAD model results over the North-Atlantic with CRISTA-2 data and other available measurements shows that the model produces reliable results for temperature in that region and that the mesoscale structure of water vapour is reasonably well reproduced with some bias of the calculated mixing ratios. A similar evaluation has not been carried out for the Indonesian Archipelago. Yet qualitative comparisons with radio sonde data and global scale analyses show that temperature derived with the regional model rather well resembles the observed tropical temperature field. The results for water vapour seem to show larger deviations from reality (as far as it is known). Comparison between Fig. 4.2 (based on CRISTA-2) and Fig. 4.3d (regional simulation) indicates that deviations up to a factor of 2 are possible, so that water vapour has to be regarded as a less reliably simulated quantity. The reason for the increased uncertainty is the strong vertical gradient and appreciable horizontal changes of water vapour mixing ratio in the upper tropical troposphere which are difficult to catch in numerical simulations.

4.3 Meso-scale features of the horizontal water vapour distribution during the CRISTA-2 episode

It is evident from the wind field shown in Fig. 4.3 that the southern subtropical jet (indicated by strong eastward winds in the southern part of the model domain) plays the main role for the formation of elongated cloud bands, i. e. TPs, during the analysed episode. The jet takes up moisture transported around the dry air mass south of Sumatra and Java by an equatorial easterly flow anticyclonically turning southward a few hundred kilometres west of Java. Actually, two phases of TP formation can be seen. On August 4 a first cloud band forms (Fig. 4.3a,b). It loses its shape around August 10 (Fig. 4.3c). On August 12 a new TP develops (Fig. 4.3d). This one exists until the end of the episode on August 16 (Fig 4.3e,f). Such TPs advect large amounts of moist tropical air into the mid-latitudes. The prominent intrusion of dry air first identified by CRISTA observations may be regarded as a reverse flow from Australia towards the equator. The dry air mass can be found throughout the free troposphere as shown in Fig. 4.4 containing a vertical cross section of the dew point depression from NW to SE through the centre of the dry air mass. It is transported in a meso-scale vortex and gets gradually mixed with surrounding moister air.

The smaller scale structures (eddies) are highly variable indicating the dominant impact of convection. Apparently, they are most pronounced over the islands and coastal areas of the model domain indicating the influence of land-sea contrast and orography.

4.4 Meso-scale eddy analysis: method

Vertical eddy fluxes are an important process regarding the transport of properties of air masses. It is plausible that they are enhanced in regions with strong convection like the tropics. Yet little has been done till now to quantify this process for the meso-scale. In this project the convectively highly active area marked in Fig. 4.8 has been chosen for a quantitative analysis of average eddy fluxes related to the meso-scale perturbations changing with height and time.

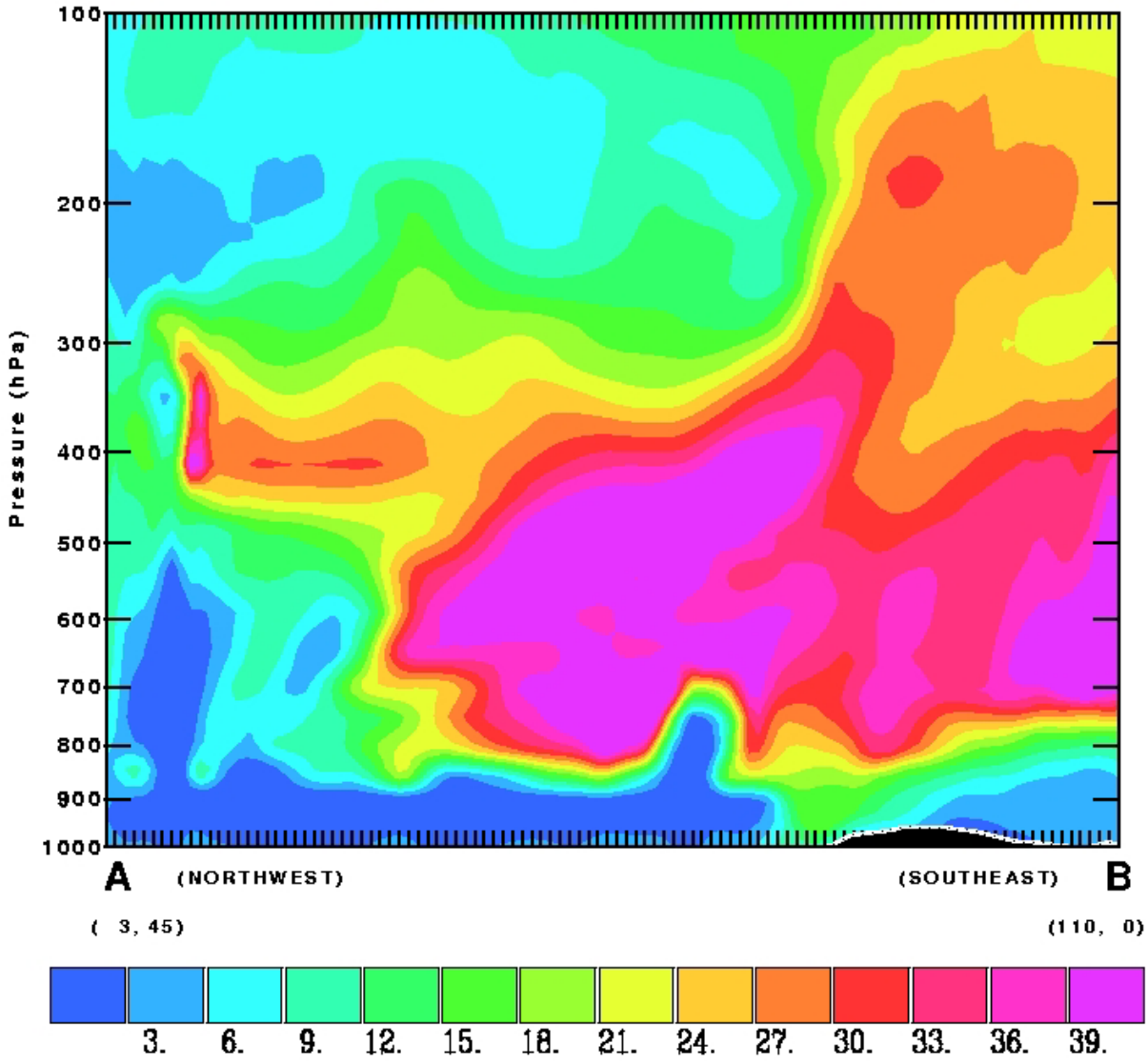

Fig. 4.4: Dew point depression in degrees K along the line shown in Fig. 4.3 for 12 August 1997, 00 UTC

A special analysis tool has been developed for this purpose. It is based on the assumption that spatial averages can be used to get a reasonable estimate of local deviations or perturbations. It is noted that this approach filters the fluctuations in a certain range of horizontal wave lengths depending on the resolution of the model (54 km in this case) and the extension of the area used for averaging (order of 1000 km). In particular, this means that wavelengths below about 100 km contribute little to the perturbation and flux estimates. This has to be kept in mind when drawing conclusions from the results.

For structural analysis the absolute value of the deviation of a quantity x from its spatial average $\bar{x}$ (Equ. 1) has been used. For better comparison of results obtained from different parameters it has been normalized according to Equ. 2. Vertical flux estimates have been carried out employing Equ. 3.

$$x'_{ij} = \left| x_{ij} - \bar{x}_{ij} \right| \qquad \text{absolute deviation} \qquad (1)$$

$$X'_{ij} = 100 \cdot x'_{ij} / \bar{x}_{ij} \qquad \text{normalised absolute deviation} \qquad (2)$$

$$F_{wy,ij} = y'_{ij} * w'_{ij}, \qquad \text{local vertical flux of y} \qquad (3)$$

$$y'_{ij} = y_{ij} - \bar{y}_{ij} \qquad \text{local perturbation} \qquad (4)$$

$$with \qquad y = H, q, \rho v_{hor}$$

The symbols ()' represent deviations of an atmospheric parameter from its spatial average (Equ. 4) in a rectangle with grid points (k,l) around a central point (i,j). *H, q,* ρ and v_{hor} stand for heat, water vapour density, air density and horizontal velocity, respectively. A rectangle of 21x21 grid boxes (1134 km x 1134 km) was chosen for derivation of moving averages.

4.5 Meso-scale eddy analysis: results

Temperature as a relatively reliably modelled parameter is used for demonstration of spatial and temporal variance of the atmosphere over Indonesia. Results for August 9 and 13, 1997, obtained for constant pressure surfaces at 400, 150 and 30 hPa have been chosen as an example (Fig. 4.5). Evidently, the temperature field is highly variable at all levels during both selected days. Structural differences are clearly enhanced by the method chosen (Equ. 1, 2). Whereas the upper two thirds of the figures exhibit a high degree of irregularity, the lower part shows large coherent structures related to the subtropical jet and tropical plume. This is especially visible in the 400-hPa maps. Apparently, non-linear variations with distance lead to larger values of the normalised variance and nicely enhance the contrast of changes in such structures like the temperature field in a jet. Since our aim is the exploration of convectively induced eddies we will mainly concentrate on the northern two thirds of the model domain.

The maps reproduced in Fig. 4.5 clearly exhibit the complex irregular structure of the eddy field with strong variability in space and time. Yet some regularities and rules seem to show up in the simulation. There are indications that perturbations originate from the land-sea contrast found in the archipelago and possibly also by orographic impact. Occasionally quasi-circular structures appear spreading from a perhaps convectively highly active centre. Such an event can be found during 13 August, around 15 UTC, west of the middle of Sumatra in all layers for which maps are shown, i. e. from the middle troposphere up to the lower stratosphere. Sequences of elongated areas with enhanced variance which seem to move slowly and whose intensity often seems to be slightly growing with height are a regular feature. They are rather prominent at 30 hPa on 13 August 15 UTC, in the northeast part of the model domain. Typical distances of such bands vary between about 500 and 1000 km. An

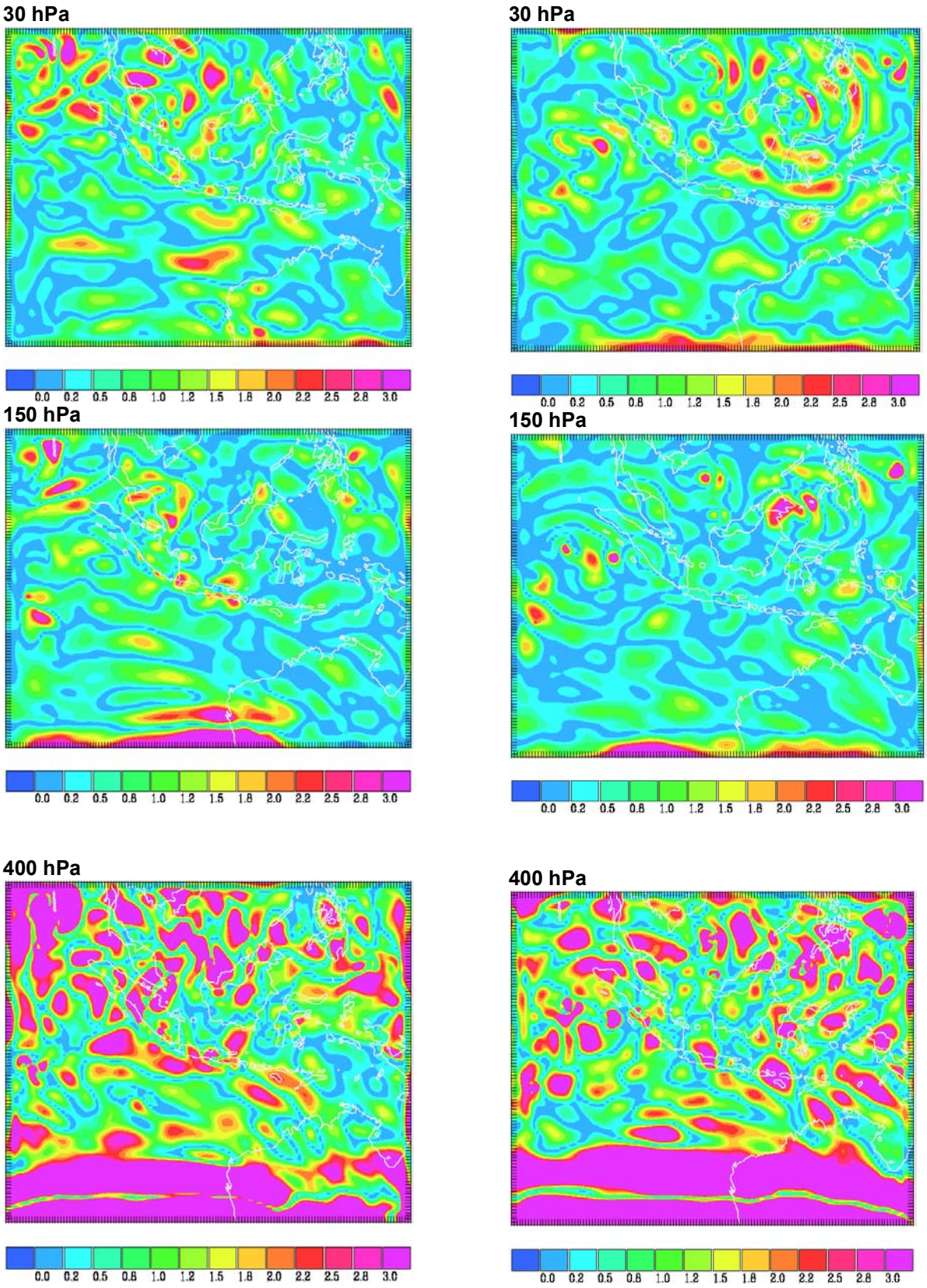

Figure 4.5: Normalised temperature deviation (Equ. 1) from gliding spatial average (21x21 gridpoints) on 30, 150, and 400 hPa constant pressure surface on August 9 (left) and 13 (right), 1997, 15 UTC.

09 UTC

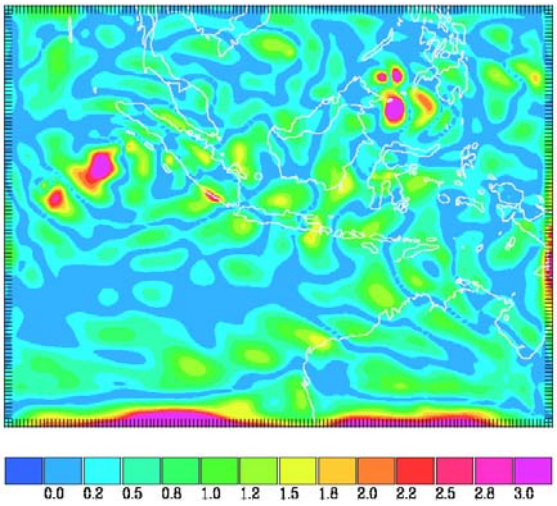

15 UTC

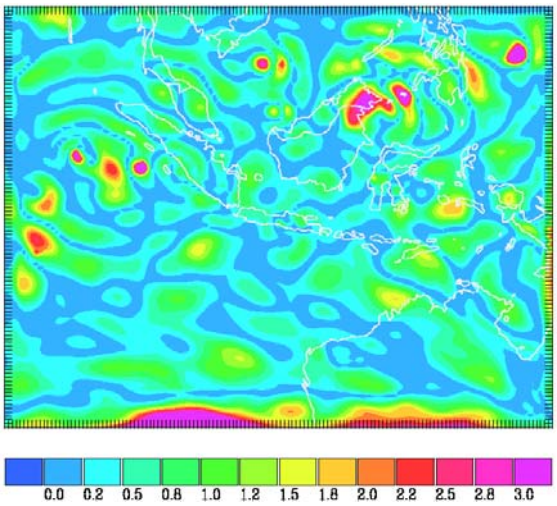

21 UTC

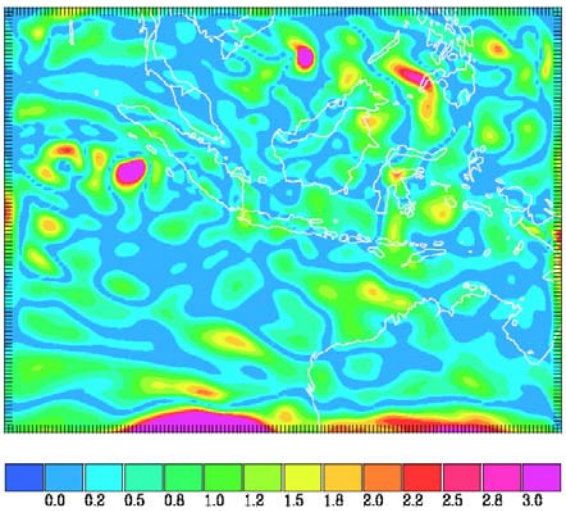

Figure 4. 6: Sequence of perturbation plots for temperature at 150 hPa constant pressure level. August 13, 1997, 09, 15 and 21 UTC (about 15, 21 and 03 LT)

A – horizontal wind perturbation

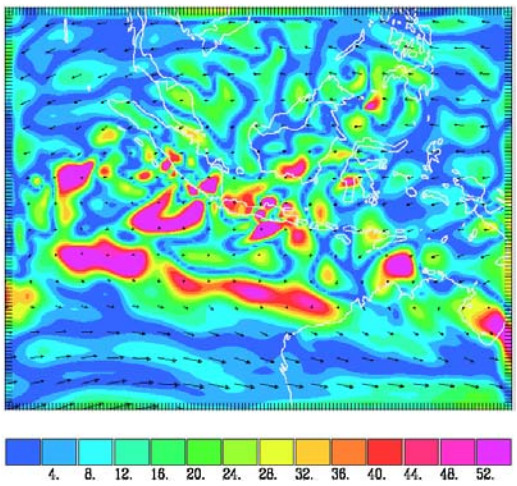

B – water vapour perturbation

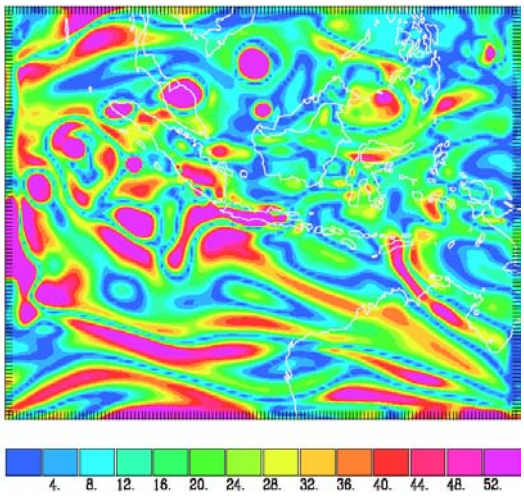

C – water vapour (ppmv)

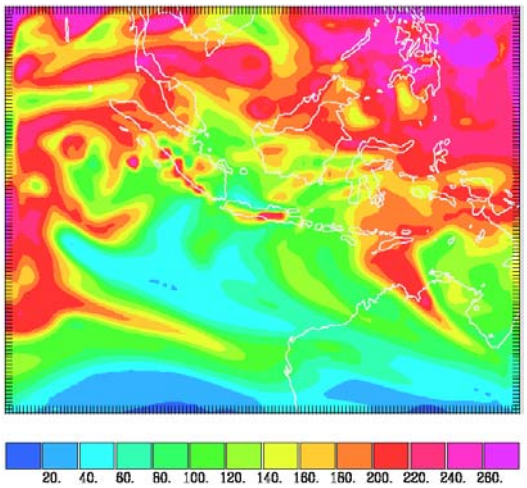

Figure 4.7:
A: Perturbation field of horizontal wind at 150 hPa, August 13, 1997, 09 UTC.
B: Perturbation field water vapour mixing ratio at 300 hPa, August 13, 1997, 15 UTC**.**
C: Mixing ratio of water vapour (ppmv) at 215 hPa, August 13, 1997, 15 UTC**.**

example of changes of the meso-scale variance on shorter time scales is given in Fig. 4.6. The mentioned centre west of Sumatra exhibits some persistence. The position of the centre is slightly oscillating. Strong temporal variability exists in the northeast corner of the domain.

Of course, the variance distribution clearly depends on the analysed quantity as it is evident from Fig. 4.7 which contains examples of perturbation fields of the horizontal wind and water vapour mixing ratio (panel A and B, respectively). The wind field exhibits strong local variability over the islands, particularly over Sumatra and Java. The orographic impact is much more visible in the horizontal wind field than in the temperature field. The widely elongated structures in the mixing ratio variance distribution in the lower half of Fig. 4.7B result from the strong gradients in the moisture field built up by the intrusion of dry air into the tropics. Panel C showing the water vapour distribution at 215 hPa has been included in Fig. 4.7 to enable easier comparison of the moisture and moisture perturbation fields.

Despite the different behaviour of horizontal variability found for different parameters it can generally be stated that the archipelago is a source of partly irregular, partly structured eddies in the upper troposphere and lower stratosphere. Furthermore, the centre of variability west of Sumatra is reflected by the variance of temperature, moisture and horizontal wind. It is connected with the centre of anticyclonic rotation of the flow as indicated by the moisture field (Fig. 4.7C) and by the horizontal wind (arrows in Fig. 4.7A).

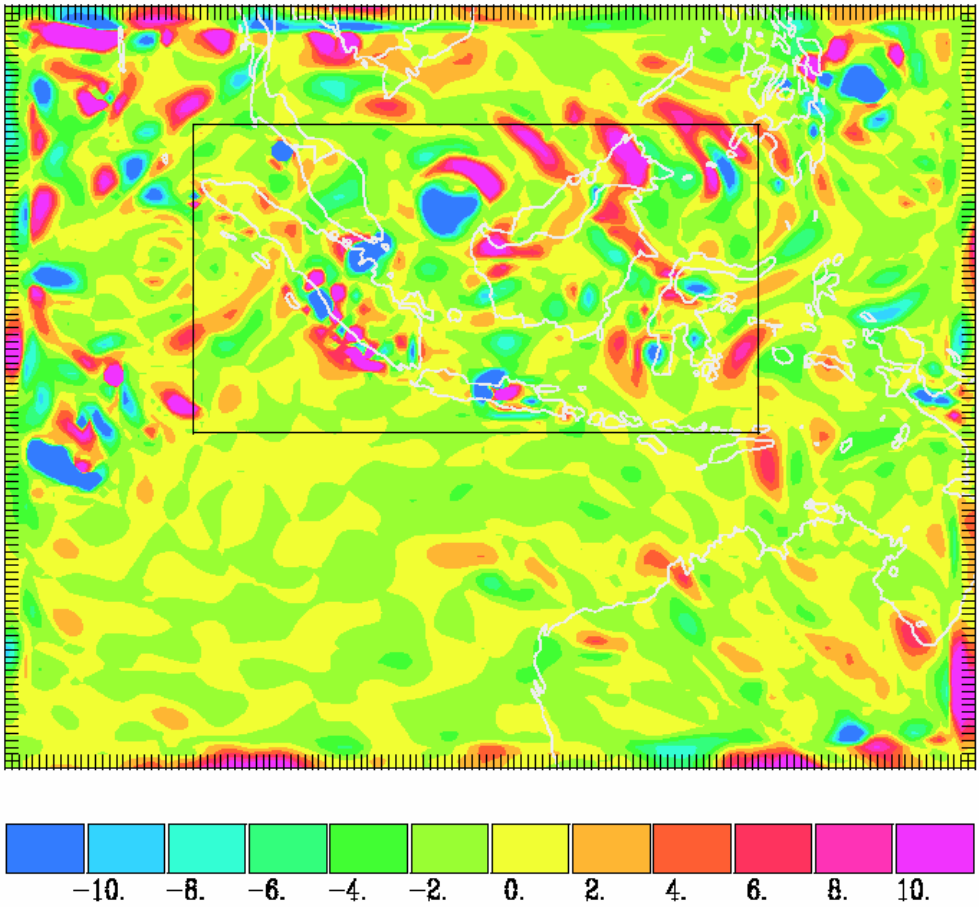

Figure 4.8: Vertical sensible heat flux (W/m²) on August 11, 1997, 06 UTC (about 12 LT) at 200 hPa. The frame marks the region for which horizontally averaged flux estimates have been derived.

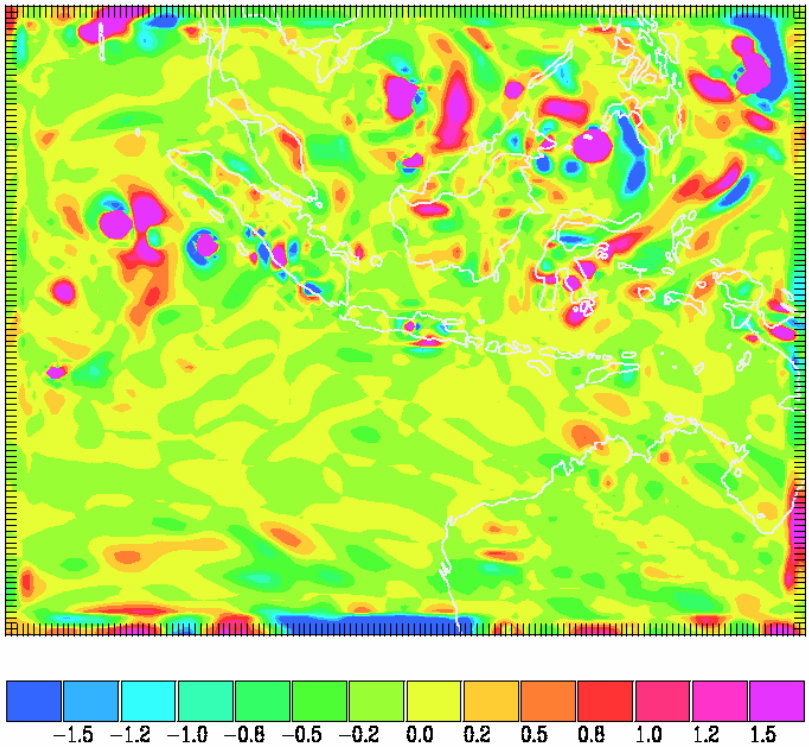

Figure 4.9: Vertical meso-scale eddy flux of sensible heat (W/m²) on August 13, 1997, 15 UTC at 300 hPa.

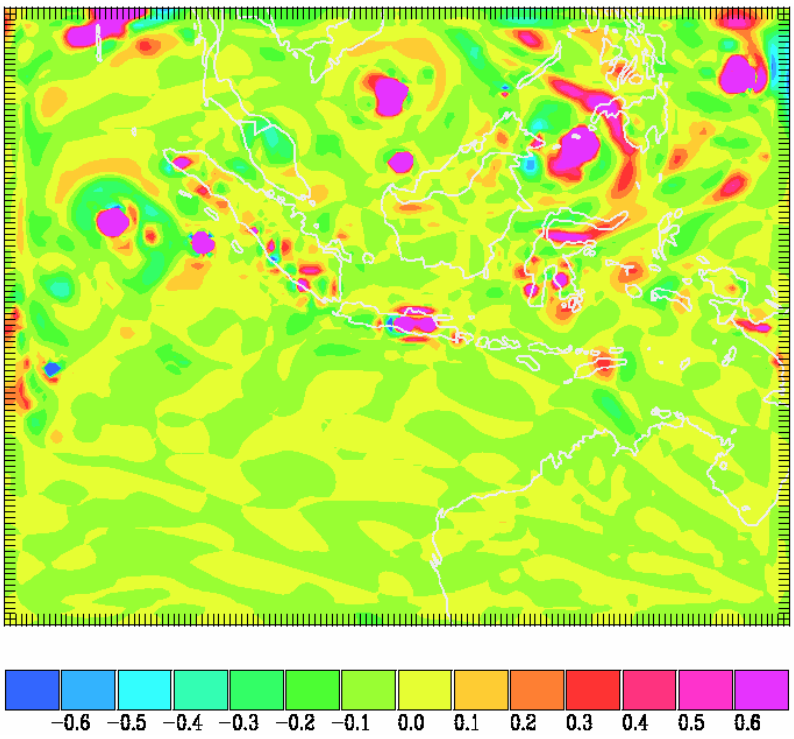

Figure 4.10: As Fig. 4.9, but for moisture.

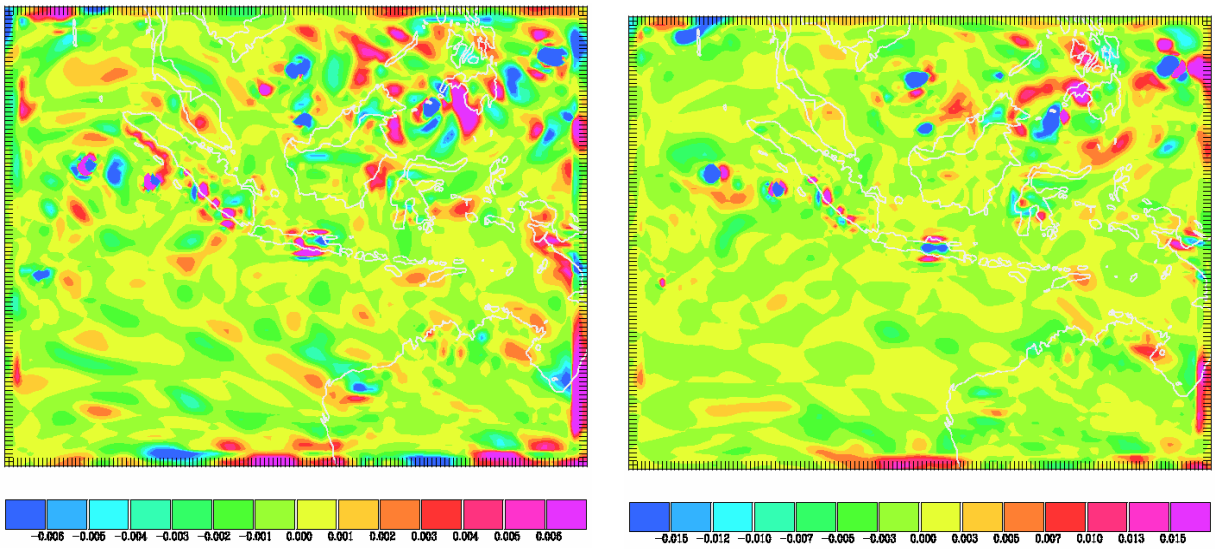

Figure 4.11: Vertical meso-scale eddy momentum flux (N/m²). August 13, 1997, 15 UTC, 300 hPa (left panel) and 215 hPa (right panel)

Elongated wavelike structures are also present in the maps of vertical meso-scale eddy flux estimates. The upper part of Fig. 4.8 showing estimates for August 11, 1997, 12 LT, at 200 hPa contains a nice example of such waves with upward and downward directed fluxes of sensible heat moving ENE away from a centre with strong downward eddy transport. (As already mentioned, the area marked by a frame is used for the estimation of spatially temporally averaged eddy fluxes.) A similar centre, but with strong upward eddy heat flux, is also found two days later (Fig. 4.9). A region of increased upward eddy flux of moisture exists at the same time and location (Fig. 4.10). It is accompanied by a clearly identifiable, but weaker centre with downward flux of water vapour over the Malaysian Peninsula. This second centre is less pronounced in the temperature flux exhibited in Fig. 9. As can be seen from comparison with Fig. 7B both centres show marked local variance. This points to the existence of a bipolar convective system, indications of which are also present in the meso-scale temperature variance (Fig 4.5). The core of the anticyclonic centre west of Sumatra proves to be a place of enhanced upward heat and moisture fluxes (Figs. 4.9, 4.10) whereas the momentum eddy transport (Fig. 4.11) varies between upward and downward fluxes on rather short spatial scales in the vicinity of the centre. Fig. 4.12 demonstrates that two of the centres are also clearly visible in the mostly flat temperature distribution and geopotential height field. The low meso-scale gradients in the tropics make it rather difficult to extract such features. The eddy momentum flux shown in Fig. 4.11 for three pressure levels, namely 300, 215 and 150 hPa, is mainly directed downward and decreasing in magnitude with increasing height during the episode, but

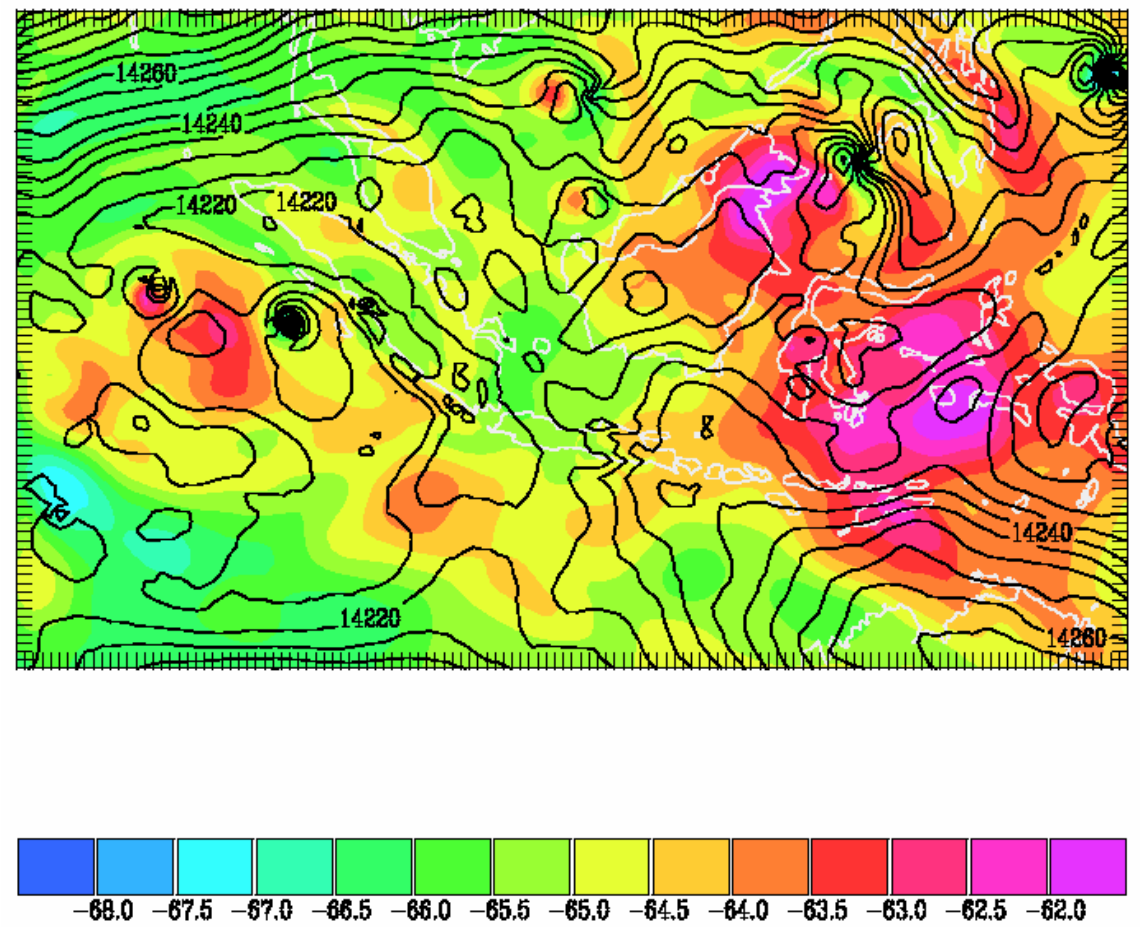

Figure 4.12: Geopotential height (in gpm, contour lines in increments of 10 gpm) and temperature (degree C, coloured contours) on the 150-hPa constant pressure surface. August 13, 1997, 15 UTC.

the principal horizontal structure of the flux field does not change too much. Apparently and sensibly, most of the eddy momentum is deposited in the troposphere and does not reach the stratosphere as the lowest layer of the middle atmosphere. It may be argued that the small fraction of the momentum flux going upward and penetrating into the stratosphere is relevant for the circulation of the middle atmosphere.

4.6 Discussion

The simulation of the meso-scale structure of the upper tropical troposphere and lower stratosphere over the Indonesian Archipelago and its vicinity reveals strong variability of all treated quantities (temperature, wind, water vapour, fluxes of atmospheric properties). It has been expected and is clearly reflected by the results that this variability is generated by convection. Yet it was not clear in advance which (secondary) processes are controlling the variability and what meso-scale eddy fluxes of properties are generated by them.

In addition to the expected variability resulting from the impact of land-sea differences and orography it is evident from the simulations discussed in the previous section that quasi-regular dynamical structures modify the otherwise highly irregular meteorological fields over the archipelago, i. e. the convectively controlled part of the model domain. Two principal types of such structures show up mainly in the variance and flux analyses, namely circular and elongated ones. It appears plausible to attribute them to convective systems and

atmospheric waves, respectively. The most probable type of waves (which can be identified with the method used to extract perturbations from the simulated fields) is internal gravity waves generated by convection. This assumption is in accordance with the observation by Preusse (2001) that the gravity wave activity in the stratosphere over Indonesia was enhanced during the CRISTA-2 episode. The appearance of bipolar structures indicates that convective systems can and obviously do interact. What is difficult to answer based on the available data is the question whether multi-polar convective fields with three or more centres do exist during the simulated episode.

Spatially averaged flux estimates have been derived for the region marked in Fig. 4.8 with most pronounced convection avoiding the region where the southern subtropical jet and the tropical plume show up. This has been done for water vapour, sensible heat and momentum. At present, there is no reliable way to verify such model calculations. We think that the calculations of eddy heat and momentum fluxes yield acceptable results regarding magnitude and temporal change in the meso-scale. In the case of water vapour the initial and boundary values taken from ECMWF and/or NCAR/NCEP analyses may contain uncertainties which can cause larger errors of the calculations as already argued above. Therefore, these results should be regarded with reservation. Yet it is noted that the simulated temporal changes appear to be quite sensible from the view point of meteorology. Despite our reservation we decided to include the results for water vapour in this report since to our knowledge it seems to be the first time that such a meso-scale flux analysis has been performed for the tropics (and elsewhere).

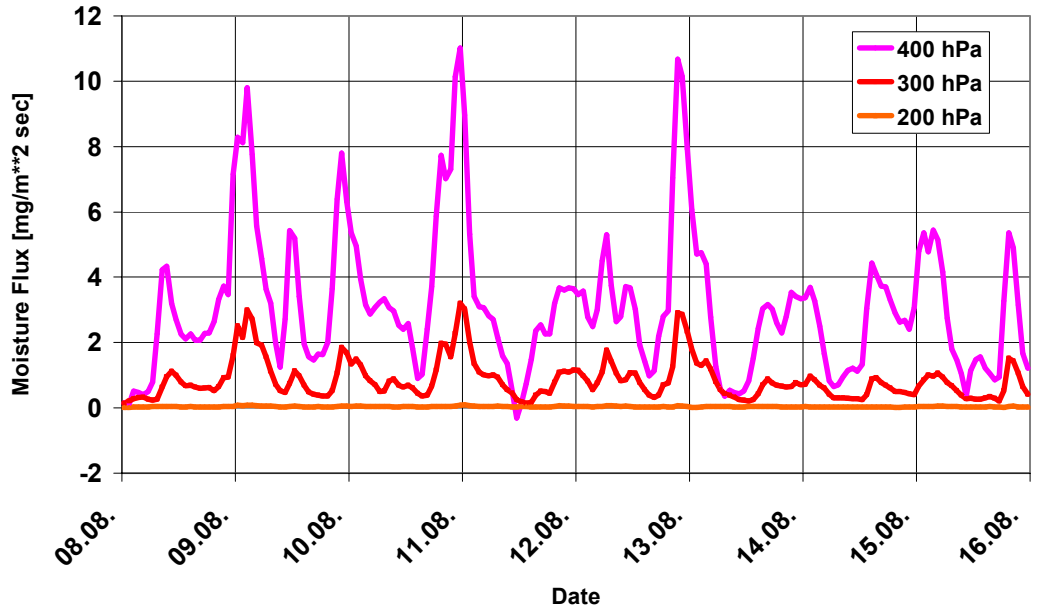

Figure 4.13: Average meso-scale eddy fluxes of water vapour (mg/m²/sec) at 400, 300 and 200 hPa in the region marked in Fig. 8 during the CRISTA-2 episode. The horizontal time scale starts at 8 August 1997, 00 UTC (06 LT).

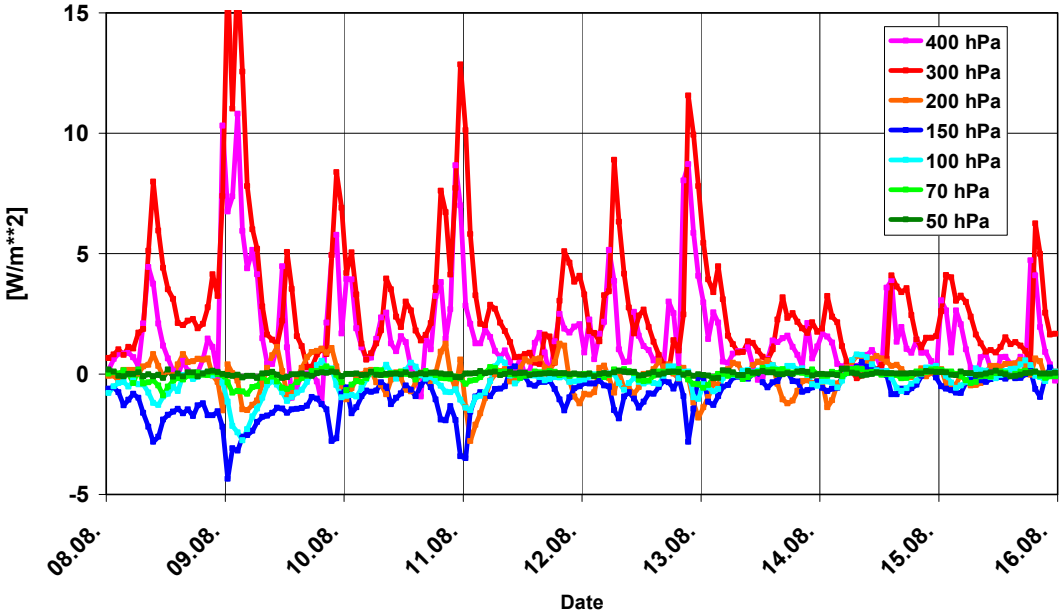

Figure 4.14: As Fig. 13, but for sensible heat flux (W/m²) between 400 and 50 hPa.

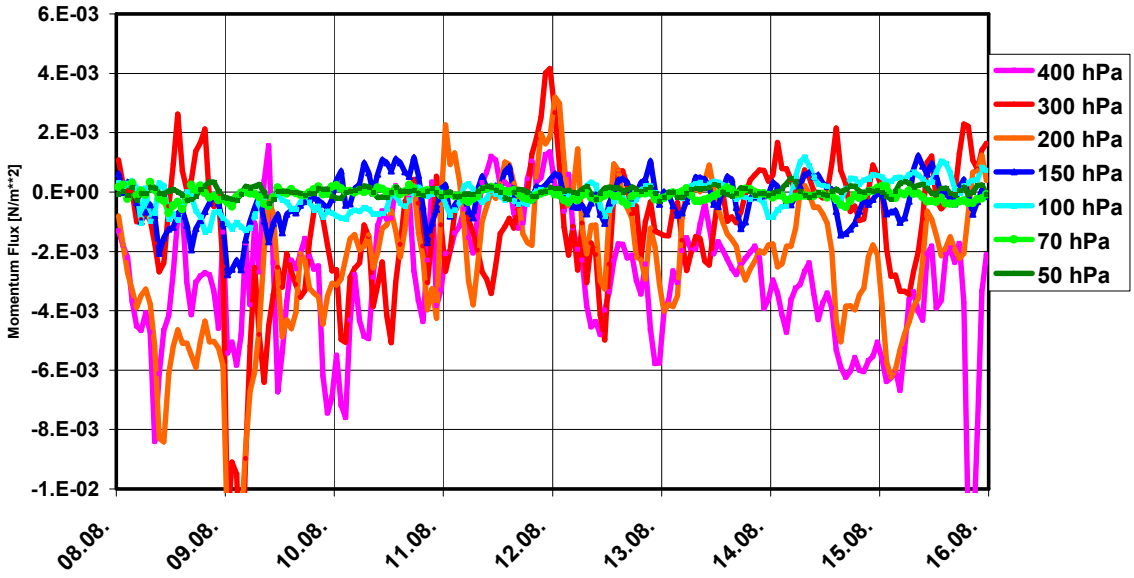

Figure 4.15: As Fig. 4.13, but for momentum flux (N/m²) between 400 and 50 hPa.

It is quite obvious from Figs. 4.13 and 4.14 that vertical eddy fluxes of water vapour and sensible heat are highly correlated up to a level of at least 300 hPa. They show relatively strong peaks during the first 6 days of the simulation period and exhibit a pronounced diurnal and reduced semi-diurnal oscillation. Except for some moments (which may be due to

shortcomings of the calculation) the vertical flux of moisture appears to be upward and convergent in the upper troposphere. This means that meso-scale eddies contribute with changing intensity to upward water vapour transport and deposition in upper levels as expected. Above 300 hPa the eddy moisture flux rapidly decreases as evident from Table 4.1.

Table 4.1: *Simulated average meso-scale eddy fluxes of momentum, sensible heat and water vapour during the CRISTA-2 episode (August 8 – 16, 1997)*

Pressure hPa	Momentum N/m^2	Heat W/m^2	Water Vapour 10^{-6} $kg/m^2/s$
400	-3.01E-03	1.67E+00	3.14E+00
300	-1.20E-03	2.92E+00	8.55E-01
200	-2.33E-03	-6.76E-02	3.96E-02
150	-2.36E-04	-8.66E-01	2.30E-03
100	-1.34E-04	-2.68E-01	2.90E-04
70	-9.72E-05	-7.85E-02	1.62E-05
50	2.25E-05	1.03E-02	

Sensible heat eddy fluxes are grossly directed upward at lower levels and downward at higher levels leading to convergence of the flux in and heating of the tropopause region. Average vertical eddy fluxes of momentum are downward at all levels except at 50 hPa and increase in magnitude with decreasing height (Table 4.1). Yet up going pulses also occur, leading to momentum transport from the troposphere into the stratosphere (which is an important factor for the general circulation of the upper atmospheric levels). The simulations give strong evidence that this process can cause as strong and more frequent momentum flow into the stratosphere over the archipelago region as estimated for gravity wave emission from severe tropical storms (around 0.3 $N \cdot m^{-2}$, Chen and Lu, 2001). Therefore, since gravity waves are involved in this process, tropical convective regions may play a more important role than assumed till now for the momentum budget of the middle atmosphere.

Conclusion

The results presented in the previous section demonstrate that the regional meteorological model MM5 (Grell et al., 1994) as used in the EURAD system is well suited to deal with the meso-scale structure of the upper tropical troposphere and lower stratosphere. It reproduces special larger scale features like an intrusion of dry air and the generation of tropical plumes which were observed by CRISTA-2 with it highly resolving hawk-eye mode reasonably well. In addition it succeeds to simulate finer scale disturbances, i. e. eddies, generated by convective activity over the Indonesian Archipelago. A simple but efficient method of analysis has been designed on the basis of variance and perturbation estimates which allows the extraction and visual enhancement of the disturbances and thus better qualitative and in the case of eddy fluxes also quantitative analysis.

It became evident that the formation of plumes observed south of the archipelago was controlled by the subtropical jet stream. Since this phenomenon is of great relevance for precipitation in some areas of (western) Australia it may be promising to conduct a special

study of this problem exploiting the high quality observations of CRISTA-2. In this study we put more weight on the investigation of convectively induced disturbances over the archipelago with the aim to contribute to a better understanding of the formation and impact of meso-scale eddies in the tropical tropopause region. It seems that our study is the first of its kind for the tropical atmosphere.

The analysis revealed the existence of a rather irregular eddy distribution over the archipelago modified by land-sea contrasts and orography. Yet there is also clear evidence of some organised structures. These have the appearance of waves and cells or centres from which such waves seem to be emitted. These structures are present in the eddy fields of all analysed parameters, namely temperature, horizontal wind and mixing ratio of water vapour. A bipolar cell system could be identified in the perturbation maps shown in this study. It is plausible to assume that the eddies are generated by convection over the archipelago. And it is hypothesised that the wavelike structures are an indication of internal gravity wave generation by convection.

Local vertical eddy fluxes of sensible heat, water vapour and momentum were estimated and integrated over the area with strongest convective activity. Calculated water vapour fluxes are regarded to be less reliable but have been included in the discussion because they exhibit interesting and sensible meteorological features. During the analysed episode strong positive correlation exists between the temporal variation of heat and moisture eddy fluxes at the lower analysed levels (up to 300 hPa). Both exhibit a pronounced diurnal and somewhat weaker semi-diurnal oscillation during most of the time of the analysed period. As a marginal remark we would like to state that this may play a role for the generation of tidal oscillations in the upper part of the middle atmosphere. Most of the heat and water vapour transported upward from lower layers by eddies does not leave the troposphere. Momentum eddy fluxes which are directed downward on the average during the episode, may nevertheless add up to up going pulses which can propagate into the middle atmosphere. The calculations show that they can reach the same intensity when integrated over larger regions like the archipelago as gravity wave emissions from severe tropical storms with smaller extension. They may therefore significantly contribute to the control the general circulation of the middle atmosphere.

5 References

Ancellet G., Pelon J., Beekmann M., Papayannis A. und Megie G.: Ground-based lidar studies of ozone exchange between the stratosphere and the troposphere. J. Geophys. Res. 96, 22401 – 22421, 1991.

Ancellet, G., M. Beekmann and A. Papayannis: Impact of a cutoff low development on downward transport of ozone in the troposphere. J. Geophys. Res. 96, 22401 – 22421, 1994

Beekmann, M., G. Ancellet, S. Blonsky, D. de Muer, A. Ebel, H. Elbern, J. Hendricks, J. Kowol, C. Mancier, R. Sladkovic, H. G. J. Smith, P. Speth, T. Trickl and Ph. van Haver; Regional and global fold occurence and related ozone flux across the tropopause, *J. Atmos. Chem.* 28, 29 – 44, 1997.

Berggren, R., B. Bolin, and C.-G. Rossby: An aerological study of zonal motion, its perturbations and breakdown. Tellus 1 (2), 14-37, 1949.

Benzi, R., B. Saltzman and A. Wiin-Nielsen (eds.): *Anomalous Atmospheric Flows and Blocking.* Advances in Geophysics, Vol. 29, Academic Press, 459 pp., 1986.

Chen, Z., and D. Lu, Numerical simulation of stratospheric gravity waves above mid-latitude deep convection, Adv. Space Res., 27, 1659 – 1666, 2001.

Ebel A., Hass H., Jakobs H. J., Memmesheimer M., Laube M., Oberreuter A., Geiss H. und Kuo Y.-H.: Simulation of ozone intrusion caused by a tropopause fold and a cut-off low. Atmos. Environment 25A, 2131 – 2144, 1991

Ebel, A., H. Elbern, J. Hendricks and R. Meyer; Stratosphere-troposphere exchange and its impact on the structure of the lower stratosphere, *J. Geomag. Geoelectr.*, 48, 135-144, 1996.

Ebel A., H. Elbern, H. Feldmann, H. J. Jakobs, Ch. Kessler, M. Memmesheimer, A. Oberreuter and G. Piekorz; Air pollution studies with the EURAD model system (3): EURAD–European Air Pollution Dispersion model system*, Mitteil. Inst. Geophys. Meteor. Universität zu Köln*, no. 120, 1997.

Elbern, H., J. Kowol, R. Sladkovic und A. Ebel: Deep stratospheric intrusions: A statistical assessment with model guided analyses. Atmos. Environment., 31, 3207-3226, 1997

Elbern, H., J. Hendricks und A. Ebel: A climatology of tropopause folds by global analyses. Theor. Appl. Climatol., 59, 181-200, 1998

Emmons, Louisa K., Didier A. Hauglustaine, Jean-Francois Muller, Mary Anne Carroll, Guy P. Brasseur, Dominik Brunner, Johannes Staehelin, Valerie Thouret, Alain Marenco, Data composites of tropospheric ozone and its precursors from aircraft measurements, J. Geophys. Res., 105, 20,497-20,538, 2000.

Flatoy F. und Hov O.: Model studies of the effects of aircraft emissions in the North Atlantic flight corridor during October 26 - November 13, 1994, and June 18 - July 5, 1995, in: U. Schumann (Herausg.), Contribution to the Final Report of the POLINAT Project, Commission of the European Communities, 1996

Grewe V. und Dameris M.; Calculating the global mass exchange between stratosphere and troposphere, *Annales Geophys.* 14, 431 – 442, 1996.

Fournier, A.: Atmospheric energetics in the wavelet domain.Part II: Time-averaged observed atmospheric blocking. *J. Atmos. Sci.* 60, 319 – 338, 2003.

Grell, G., J. Duddhia, and D. Staufer: A description of the fifth-generation Penn State/Ncar meso-scale model (MM5), *Technical note NCAR/TN-398+STR*, National Center of Atmospheric Research, Boulder, 1994.

Grewe V. und Dameris M.; Calculating the global mass exchange between stratosphere and troposphere, *Annales Geophys.* 14, 431 – 442, 1996.

Hass, H., A. Ebel, H. Feldmann, H.J. Jakobs, M. Memmesheimer: Evaluation studies with a regional chemical transport model (EURAD) using air quality data from the EMEP monitoring network. Atmospheric Environment, 27A, 867-887, 1993.

Hendricks J.: Modellstudien zur Bedeutung heterogener Reaktionen auf und in Sulfataerosolen für die Photochemie der Tropopausenregion mittlerer Breiten. Mitteil. Inst. Geophys. Meteor. Universität zu Köln, Heft 122, 1997

Holton J. R., P. H. Haynes, M. E. McIntyre, A. R. Douglas, R. B. Rood and L. Pfister; Stratosphere-troposphere exchange, *Rev. Geophys.* 33, 403 – 409, 1995.

Kalnay, E. M. Kanamitsu, R. Kistler, W. Collins, D. Deaven, L. Gandin, M. Iredell, S. Saha, G. White, J. Woollen, Y. Zhu, M. Chelliah, W. Ebisuzaki, W.Higgins, J. Janowiak, K. C. Mo, C. Ropelewski, J. Wang, A. Leetmaa, R. Reynolds, Roy Jenne, Dennis Joseph: The NCEP/NCAR 40-Year Reanalysis Project. Bull. Amer. Meteor. Soc., 1996, 77,437-431. 1996.

Kley, D., J. M. Russel III, and C. Phillips, SPARC assessment of upper tropospheric and stratospheric water vapour, WCRP 113, WMO/TD No. 1043, SPARC Rep. No. 2, 2000.

Kowol-Santen, J., H. Elbern and A. Ebel; Estimation of cross-tropopause air mass fluxes at midlatitudes: comparison of different numerical methods and meteorological situations, *Mon. Wea. Rev.* 128, 4045 – 4057, 2000.

Kuhnelt, I.; Tropical-extratropical cloud bands in the Australian region, *Intern. J. Climatol.* 10, 341 – 364, 1990.

Lippert E.: Der Einfluss von Flugzeugabgasen auf die Atmosphäre: Untersuchungen mit einem mesoskaligen Chemie-Transport-Modell. Mitteil. Inst. Geophys. Meteor. Universität zu Köln, Heft 109, 1996

MacKenzie, R., K. Carslaw, J. Ström, Th. Peter und L. Stefanutti: Tropical convection and stratospheric chemistry – The objective of APE-THESEO, in: K.S. Carslaw and G.T. Amanatidis, eds., Mesoscale Processes in the Stratosphere, European Communities, Air Pollution Res. Rep. 69, EUR 18912 en, pp. 153-158, 1999.

McGuirk, J. P. Thompson, A.H., Smith, N.R.: Moisture bursts over the tropical Pacific Ocean. Mon. Wea. Rev., 115, 787-798, 1987.

Memmesheimer, M., H.J. Jakobs, H. Feldmann, G. Piekorz, Ch. Kessler, E. Friese, A. Ebel: Computergestützte Langzeitsimulationen zur Bewertung von Strategien zur Luftreinhaltung. Abschlußbericht, 29. November 2000.

Newman, P.A., D. W. Fahey, W.H. Brune, M.J. Kurylo und S.R. Kawa: POLARIS (Preface to Special Section), J. Geophys. Res., 104, 26.481-26.495, 1999.

Offermann, D., K.U. Grossmann, P. Barthol, P. Knieling, M. Riese, and R. Trant; The CRyogenic Infrared Spectrometers and Telescopes for the Atmosphere (CRISTA) Experiment and Middle Atmosphere Variability; J.Geophys.Res., 104, 16,311-16,325, 1999.

Offermann, D., M. Jarisch, B. Schaeler, G. Eidmann, M. Langfermann, J. Oberheide, T. Wiemert, M. Riese, and C.Schiller, Trace gas densities and dynamics at and above the tropopause as derived from CRISTA data, in: Optical Remote Sensing of the Atmosphere and Clouds II, eds. J. Wang and T. Hayasaka. Proc. of SPIE, Vol. 4150, pp. 10 – 19, 2001.

Offermann, D., B. Schaeler, M. Riese, M. Langfermann, M. Jarisch, G. Eidmann, C. Schiller, H. G. Smit and W. G. Read; Water vapor at the tropopause during the CRISTA 2 mission, J. Geophys. Res. 107 (D23), 8176, doi: 10.1029/2001JD000700, 2002

Offermann, D., K. U. Grossmann, P. Barthol, P. Knieling, M. Riese and R. Trant; The CRyogenic Infrared Spectrometers and Telescopes for the Atmosphere (CRISTA) Experiment and Middle Atmosphere Variability*, J. Geophys. Res.*, 104, 16311-16325, 1999.
Pelly J.L. and B.J. Hoskins: A new perspective on blocking. Journal of the Atmospheric Sciences, Vol 60, pp. 743-755, 2003.

Olivier, J.G.J, J.J.M Berdowski, J.A.H.W. Peters, J. Bakker, A.J.H. Visschedijk and J.J. Bloos, Application of EDGAR – Including a description of EDGAR 3.2: reference database with trend data for 1970-1995. RIVM report 773301001 / NRP report 410200051, 2001/2002.

Pelly, J.L. and B.J. Hoskins, 2003: A new perspective on blocking. J. Atmos. Sci., **60**, 743-755.

Preusse, P.; Satellitenmessungen von Schwerewellen in der mittleren Atmosphäre mit CRISTA, *Thesis WUB-DIS 2001-09, University of Wuppertal*, 2001

Ravetta, F., G. Ancellet, J. Kowol-Santen, R. Wilson et D. Nedeljkovic, *Ozone, temperature and wind field measurements in a tropopause fold: comparison with a mesoscale simulation*, MWR, 127, 2641-2653, 1999.

Rex, D.F.:Blocking action in the middle troposphere and its effect on regional climate. I. An aerological study of blocking action. Tellus, 2, 196-211, 1950a.

Rex, D.F.:Blocking action in the middle troposphere and its effect on regional climate. II. A climatology of blocking action. Tellus, 2, 196-211, 1950a.

Riese, M., R. Spang, P. Preusse, M. Ern, M. Jarisch, D. Offermann and K. U. Grossmann; Cryonegic Infrared Spectrometers and Telescopes for the Atmosphere (CRISTA) data processing and atmospheric temperature and trace gas retrieval, *J. Geophys. Res*., 104, 16349 – 16367, 1999a.

Riese, M., X. Tie, G. Brasseur and D. Offermann; Three-dimensional simulation of stratospheric trace gas distributions measured by CRISTA, *J. Geophys. Res.*, 104, 16419-16435, 1999b.

Roeben, B. J., Wolken in einem mesoskaligen Chemie-Transport-Modell: Prozessanalyse, Sensitivität bezueglich der horizontalen Aufloesung und Einfuehrung alternativer Bestimmungsverfahren. *Mitteil. Inst. Geophys. Meteor. Universität zu Köln*, no. 130, 1999.

Rose, K., and G. Brasseur: A three-dimensional model of chemically active trace species in the middle atmosphere during disturbed winter conditions, J. Geophys. Res. 96, 16387 – 16403, 1989

Schumann, U., H. Schlager, F. Arnold, J. Ovarlez, H. Kelder, O. Hov, G. Hayman, I.S.A. Isaksen, J. Staehelin und P.D. Whitefield: Pollution from aircraft emissions in the North Atlantic flight corridor: Overview on the POLINAT projects. J. Geophys. Res., 105, 3605-3631, 2000.

Spang, R., G. Eidmann, M. Riese, D. Offermann, and P. Preusse: CRISTA observations of cirrus clouds around the tropopause. J. Geophys. Res. 107, 8174, doi: 10.1029/2001JD000698, 2002

Stefanutti, L., L. Sokolov, S. Balestri, A.R. MacKenzie und V. Khattatov: The M-55 Geophysica as a platform for the Airborne Polar Experiment. J. Atmos. Ocean. Technol., 16, 1303-1312, 1999.

Thompson, A.M., H.B. Singh und H. Schlager: Introduction to special section: Subsonic Assessment Ozone and Nitrogen Experiment (SONEX) and Pollution from Aircraft Emissions in the North Atlantic Flight Corridor (POLINAT 2). J. Geophys. Res., 105, 3595-3603, 2000.

Tulet, P., V. Crassier, F. Solmon, D. Guedalia and R. Rosset: Description of the mesoscale nonhydrostatic chemistry model and application to a transboundary pollution episode between northern France and southern England. JGR, 108, D1, 4021, ACH 5, 2003.

Wirth V. und Egger J.: Diagnosing extratropical synoptic-scale stratosphere-troposphere exchange: A case study. Quart. J. R. Meteor. Soc. 125, 635, 1999.